Sediment deposition at the modern grounding zone of Whillans Ice Stream, West Antarctica

Huw J. Horgan,[1] Knut Christianson,[2] Robert W. Jacobel,[2] Sridhar Anandakrishnan,[3] and Richard B. Alley[3]

Received 25 April 2013; revised 26 June 2013; accepted 28 June 2013; published 2 August 2013.

[1] Much of the threshold behavior of marine ice sheets is thought to result from processes occurring at the grounding zone, where the ice sheet transitions into the ice shelf. At short timescales (decades to centuries), grounding zone behavior is likely to be influenced by ongoing sediment deposition, which can stabilize the grounding zone position. We present a ground-based geophysical study across the modern grounding zone of Whillans Ice Stream. Within an embayment setting, where subglacial meltwater drains, we image sedimentary deposits; however, we do not observe the classic asymmetric grounding zone wedge deposits, which are found in the paleorecord and are thought to stabilize the grounding zone position. At an adjacent peninsula, we image the grounding zone and an ice-shelf pinning point and again observe no wedge deposits. **Citation:** Horgan, H. J., K. Christianson, R. W. Jacobel, S. Anandakrishnan, and R. B. Alley (2013), Sediment deposition at the modern grounding zone of Whillans Ice Stream, West Antarctica, *Geophys. Res. Lett.*, *40*, 3934–3939, doi:10.1002/grl.50712.

1. Introduction

[2] The West Antarctic Ice Sheet (WAIS) is the Earth's only extant marine ice sheet, and its stability in the face of anticipated climate change is uncertain [*Joughin and Alley*, 2011]. Glaciological attention has long been focused on the WAIS's grounding zone [e.g., *Shabtaie and Bentley*, 1987], where the grounded ice sheet transitions into the floating ice shelf. This is due to a long-standing instability hypothesis [*Weertman*, 1974], which states that an ice sheet grounded well below sea level on a reverse sloping bed (a bed that slopes toward the ice sheet's interior) should undergo continuous grounding zone retreat unless stabilized by additional factors such as drag from ice shelves. More recently, this instability hypothesis has been shown to be valid when the base of the ice is sliding [*Schoof*, 2007], and several additional processes that may influence the grounding zone position have been identified [*Alley et al.*, 2007; *Gomez et al.*, 2010; *Jamieson et al.*, 2012]. However, most of the current understanding of grounding zones has been derived from modeling studies, the paleorecord, and remote sensing observations, with field-based observations of contemporary grounding zone systems relatively scarce [e.g., *Jacobel et al.*, 1994; *Smith*, 1996; *Anandakrishnan et al.*, 2007; *Catania et al.*, 2010; *MacGregor et al.*, 2011] and no comprehensive view of a modern grounding zone available.

[3] Glaciers and ice sheets are both influenced by, and modify, their substrate. This interplay is nowhere more apparent than on Whillans Ice Stream (WIS) in West Antarctica, where fast flow is enabled by a meters-thick till layer [*Blankenship et al.*, 1986], which deforms in response to shear stress exerted by the overriding ice [*Alley et al.*, 1986; *Kamb*, 2001]. This till deformation conveys sediment downstream, and together with sediment carried englacially and then melted out beneath the ice shelf [*Christoffersen et al.*, 2010], plus any sediment carried by subglacial meltwater streams, contributes to the deposition of a grounding zone system [*Alley et al.*, 1989]. These prograding till systems are often noted in the paleorecord [e.g., *Dowdeswell and Fugelli*, 2012], where they are interpreted as marking the seaward extent of flowing, grounded ice. The buildup of grounding zone wedges can provide a means of self-stabilization of the grounding zone position [*Anandakrishnan et al.*, 2007; *Alley et al.*, 2007] and introduce threshold behavior wherein the grounding zone position remains static until sufficient sea level or ice thickness change leads to rapid migration.

[4] We examined the modern grounding zone of WIS using active source seismic and kinematic GPS methods. We located our main study in an embayment of the grounding zone [*Rignot et al.*, 2011; *Bindschadler et al.*, 2011], where the outflow of water from the active subglacial lake system [*Fricker et al.*, 2007; *Horgan et al.*, 2012; *Christianson et al.*, 2012] beneath WIS is suspected to occur [*Carter and Fricker*, 2012] (Figure 1). Here we focus on sediment deposition at the grounding zone. We show that sediment till lobes are present at the grounding zone of WIS. However, these deposits are forming nearly flat-topped deposits beneath the nearly horizontal base of the ice shelf, suggesting there are additional processes contributing to the observed stability of the grounding zone [*Horgan and Anandakrishnan*, 2006].

2. Methods

2.1. Kinematic GPS

[5] The location of the grounding zone is often determined using the landward extent of discernible vertical tidal motion [*Gray et al.*, 2002; *Horgan and Anandakrishnan*, 2006; *Brunt et al.*, 2010]. Here we use a kinematic GPS survey in a manner similar to *Vaughan* [1995] to assess vertical

[1]Antarctic Research Centre, Victoria University of Wellington, Wellington, New Zealand.
[2]Department of Physics, St. Olaf College, Northfield, Minnesota, USA.
[3]Department of Geosciences, and Earth and Environmental Systems Institute, Pennsylvania State University, University Park, Pennsylvania, USA.

Corresponding author: H. J. Horgan, Antarctic Research Centre, Victoria University of Wellington, Wellington, New Zealand. (huw.horgan@vuw.ac.nz)

0094-8276/13/10.1002/grl.50712

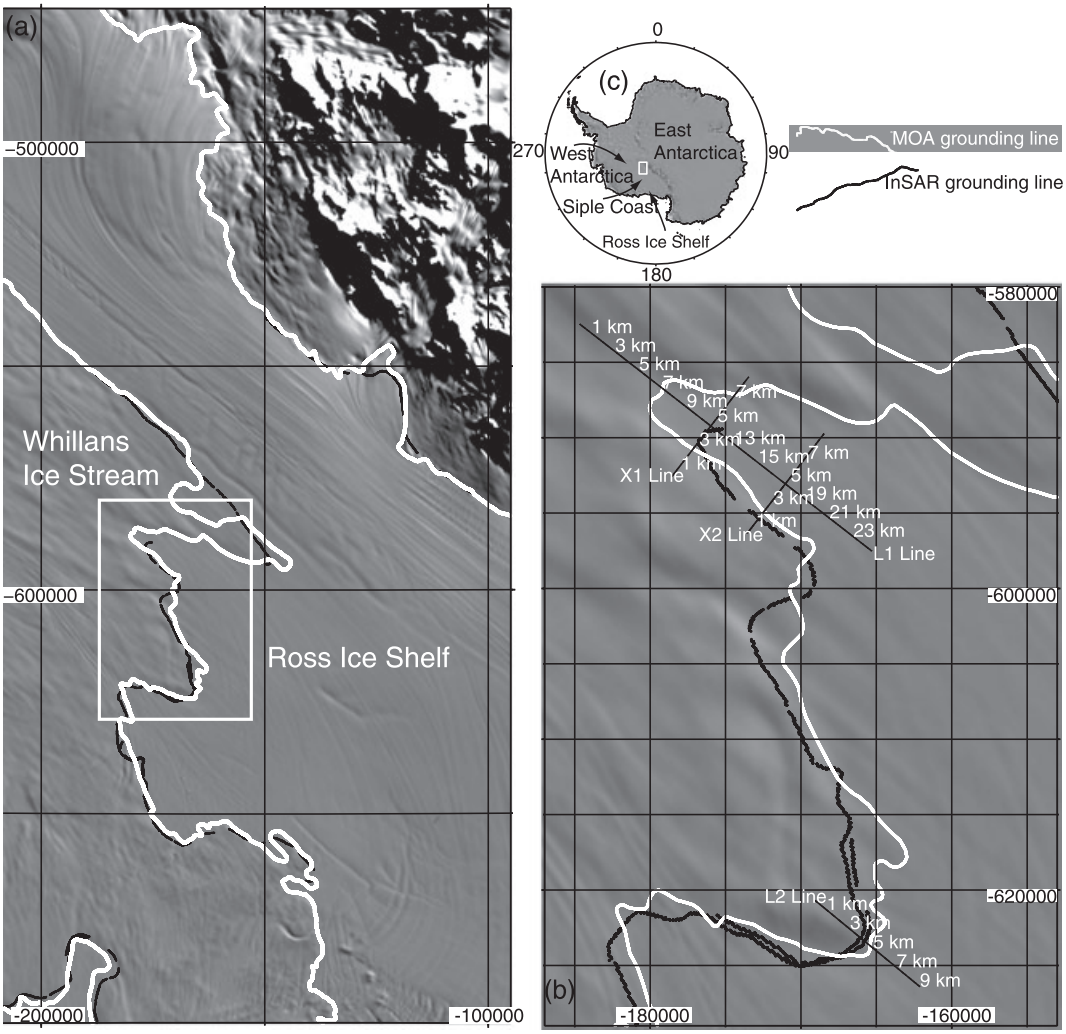

Figure 1. (a) Whillans Ice Stream, West Antarctica. Background imagery from the MODIS Mosaic of Antarctica (MOA) [*Haran et al.*, 2005]. Solid white line denotes the MOA grounding zone [*Haran et al.*, 2005]. Solid black line denotes the grounding zone of *Rignot et al.* [2011]. (b) Inset showing study location. Grounding lines as in Figure 1a. Seismic profiles are shown in black with kilometer distances in white. (c) Overview map showing the location of Figure 1a in West Antarctica.

motion along our seismic profiles during the diurnal tidal cycle. We drove the along-flow seismic profiles at approximately 20 km h^{-1}, while sampling at 1 Hz, for a sample spacing of approximately 5–6 m. This was repeated once an hour for 12 h. Data processing was performed using differential positioning techniques implemented in the software Track [*Chen*, 1998]. To examine the vertical range, we first subtracted a single best-fitting spline function from all the data, then calculated the standard deviation of the vertical position within 50 m along-track bins (Figures 2a, and 2d).

2.2. Active Source Seismic Profiling

[6] Active source seismic data were acquired along four profiles totaling approximately 50 km. One along-flow and two across-flow profiles were located in an embayment of the grounding zone (Figures 1–2). We also acquired an along-flow profile near the midline of a peninsula of the grounding zone (Figures 1–2). Small explosive charges (0.4–0.8 kg) provided the seismic source. These were buried at approximately 27 m depth at a nominal spacing of 240 m along each profile. Data were recorded on a 96-channel Geometrics Geode system. Geophones were spaced at 20 m intervals and consisted of alternating 40 Hz single phones and five-element phones housed in a single rigid plastic body. All geophones were buried approximately 0.5 m beneath the surface. Seismic data processing to produce stacked sections (Figures 2b, 2c, 2e) consisted of standard multichannel methods and included predictive deconvolution, residual-static correction, and migration.

3. Results

3.1. Embayment

[7] The onset of floatation is visible in the GPS data as an increase in the standard deviation of binned elevations downstream of km 9 (Figure 2a). In the seismic data, a high-amplitude negative reflection event is observed everywhere the ice shelf is floating during at least part of the tidal cycle (Figures 2a, 2b, km 9—line end). Beneath fully grounded ice, the ice-bed interface varies spatially and is marked by a weak negative or barely discernible reflection event, indicating very little contrast in acoustic impedance. The ocean water column thickens gradually downstream from km 9

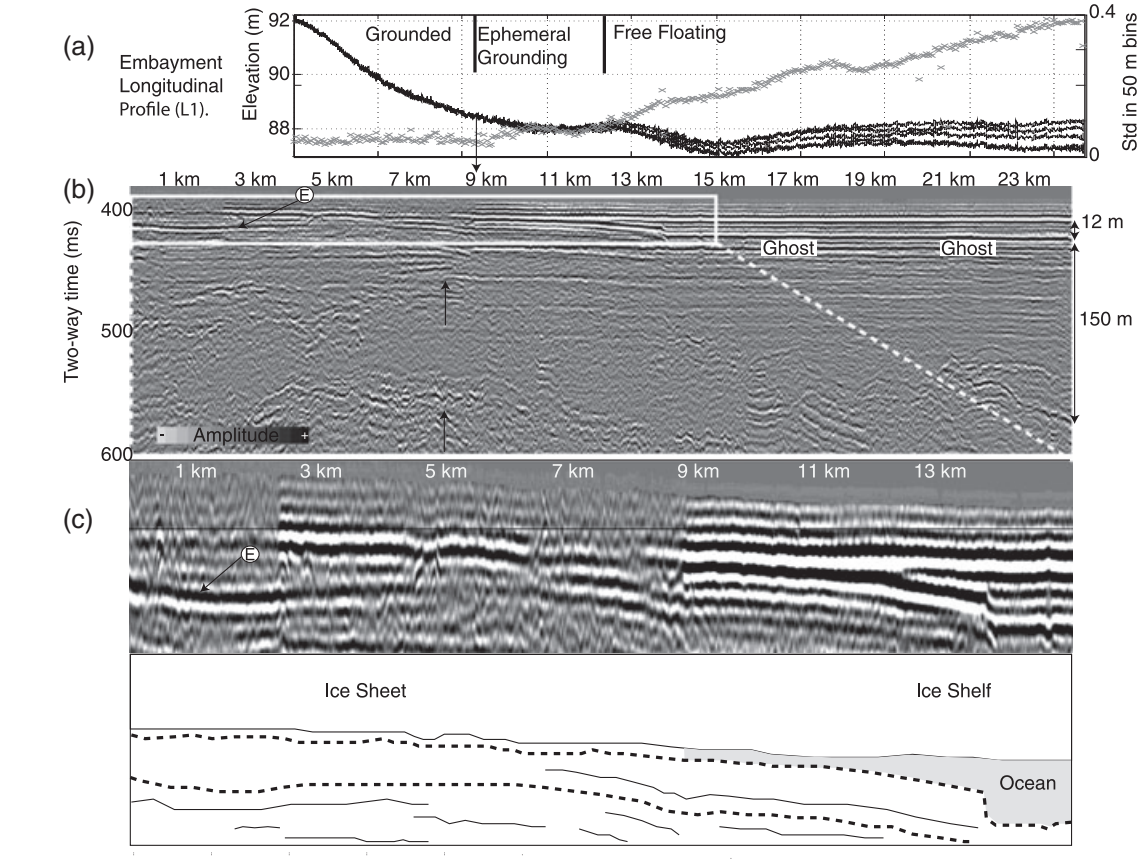

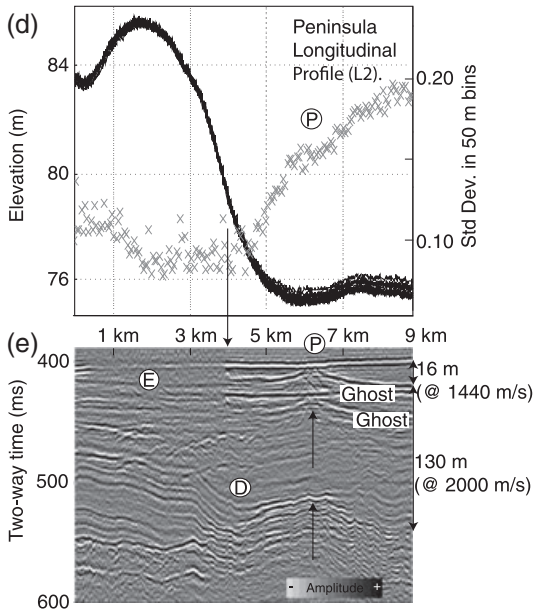

Figure 2. (a) Embayment longitudinal profile (L1) repeat kinematic GPS elevations (black lines, left axis) and bin standard deviations after the removal of a best-fitting spline function (grey crosses, right axis). (b) L1 profile active source seismic data. Upward pointing arrows highlight regions of positive topography. Downward pointing arrow marks the start of ocean water at the bed. E denotes a prominent reflector in sub-ice sediment package. (c) Zoom of sub-bed seismic stratigraphy with corresponding interpretation. Dashed lines denote sequence boundaries, solid lines denote horizons. E denotes prominent reflector in sub-ice sediment package discussed in text. (d) Peninsula longitudinal profile (L2) repeat kinematic GPS elevations (black lines, left axis) and bin standard deviations after the removal of a best-fitting spline function (grey crosses, right axis). (e) L2 profile active source seismic data. Upward pointing arrows highlight regions of positive topography. Downward pointing arrow marks the start of ocean water at the bed. E and P respectively denote the prominent reflector in sub-ice sediment package and the pinning point discussed in the text. D denotes downlapping horizons.

to 12.4, resulting in a zone of ephemeral grounding, which corresponds to a constant value in the GPS standard deviation data. Beyond km 12.4, the ocean column thickens more quickly with an abrupt step to approximately 11 m thickness at km 13.9, approximately 5 km seaward of the initial point of floatation. The water column then remains relatively constant with a thickness of approximately 12 m at the end of the along-flow line.

[8] Seismic stratigraphy beneath the ice-bed interface shows some evidence that supports recent sedimentation at the grounding zone embayment (Figures 2b, 2c). We interpret the record as showing that the most recent sedimentation results in the zone of ephemeral grounding (km 9–12.4) and the step in the bathymetry at km 13.9. (Note the strong shot-ghost approximately 25 ms beneath the bottom of the ice. This is generated by the burial of the seismic source and is sufficiently deep so as not to obscure any key features.) Sedimentation at the grounding zone is accommodation-space limited, due to the overriding ice shelf, and the bathymetric slope is away from the grounding zone. Upstream of the

grounding zone, approximately 10 ms (8 m at 1600 m s^{-1}) below the ice-bed interface, an intermediate-amplitude positive return is evident (marked E in Figures 2b, 2c). This horizon is conformable with the ice-bed interface. Within the sequence bounded by this horizon and the ice-bed interface, there is some suggestion of downlapping and toplapping beds (Figure 2c). A region of positive topography underlies the grounding zone at greater depth. Beneath this buried high, a chaotic package of reflectors is observed.

[9] Deposits seen in the cross profiles (not shown here) are in keeping with those imaged in the along-flow profile. The upstream cross profile shows a laterally continuous subglacial reflector similar in character to the lower sequence-boundary reflector on the longitudinal profile (marked E in Figure 2).

3.2. Peninsula

[10] Along the peninsula, the ice-bed interface at the upstream end of the profile (km 0–0.5) consists of a high-amplitude negative-polarity return (Figure 2e), which corresponds to a slope reversal observed in the GPS surface elevation data (Figure 2d). Moving downstream, the ice-bed interface return is then low amplitude until the ice goes afloat at km 3.9, indicated by the sudden onset of a high-amplitude bed return that approximately corresponds with an increase in the standard deviation of binned GPS elevations. Beyond km 3.9, a shallow ocean water column (less than 10 m) exists between the grounding zone and a pinning point at km 6–6.3. Pinning occurs at this location during low tide as evident in the flattening of the GPS standard deviation (Figure 2d). Beyond the pinning point, the ocean cavity thickens to approximately 16 m at the downstream end of the profile. The peninsula along-flow profile lacks the near-surface depositional features evident in the embayment. Beneath the ice-bed interface, a mix of coherent and chaotic reflection horizons is apparent above a high-amplitude coherent reflection horizon between 540 (km 2.3) and 490 ms (km 6.3). Overlying horizons downlap (labeled D in Figure 2d) onto this surface, which also forms a zone of positive topography beneath the pinning point (km 6–6.3).

4. Discussion

[11] Kinematic GPS and active source seismic data provide a detailed view of the modern grounding zone of WIS in two locations. The transition between the ice stream and the ice shelf is marked by an abrupt change in the amplitude of the basal seismic-reflection (Figures 2b, 2c, 2e), which is coincident with the onset of vertical tidal motion as imaged by repeat kinematic GPS surveying (Figures 2a, 2d). The GPS data also help highlight zones of ephemeral grounding both close to the embayment grounding zone (Figure 2a, km 9–12.2) and at the peninsula pinning point (Figure 2d, km 6.0–6.3). (We note that a similar change in the GPS standard deviation occurs at km 18 in Figure 2a, likely in response to a change in surface roughness.) The ocean water column is less than 16 m throughout the study area.

[12] In the embayment, seismic stratigraphy indicates that prograding sedimentation may be occurring. (We interpret the sea-floor bathymetric step as an active front of a sedimentary lobe (Figures 2b, 2c, km 13.8)). A prominent sub-bottom reflector (marked E in Figure 2c,) forms a lower sequence boundary at a depth of approximately 11 m beneath the ice-bed interface (based on a velocity of 1600 m s^{-1}). Similar sub-bottom reflection horizons have been observed elsewhere beneath WIS [*Rooney et al.*, 1987] and are thought to mark the bottom of a saturated unconsolidated layer [*Blankenship et al.*, 1986], which is thought to deform [*Alley et al*., 1986; 1987] thus enabling the rapid flow of WIS. A similar reflection event is visible on the upstream cross line (not shown here) at a depth of approximately 19 m. If this reflector does mark the base of the deforming layer, it is considerably thicker than previously observed [*Blankenship et al.*, 1986; *Rooney et al.*, 1987]. Alternatively, this reflector may represent deposition from a deforming layer above an older surface. Beneath this largely coherent surface, several chaotic reflection packets are observed at depth (Figure 2b). These chaotic horizons are thought to result from the delivery of unsorted diamict debris [*Dowdeswell and Fugelli*, 2012] and form a region of positive topography similar to that observed in seismic records of many paleo-grounding zone deposits around the Greenland margin [*Dowdeswell and Fugelli*, 2012]. It is possible that this topography caused the initial halt of the grounding zone in this location, and subsequent grounding zone deposition followed.

[13] At the peninsula (Figures 2d, 2e), the high-amplitude negative-polarity ice-bed interface at the start of the profile (0–0.5 km) is likely due to water trapped by the hydropotential low resulting from the surface slope reversal evident in the GPS data. The reflection from the ice-bed interface between this zone and the floatation point (km 3.9) is low amplitude. Most internal reflections appear concordant, with the exception of a chaotic package and downlapping features (Figure 2e). Seaward of the peninsula grounding zone, a topographic high leads to grounding during a portion of the tidal cycle (km 6.0–6.3). The present grounding zone floatation point (km 3.9) corresponds to a small step in the sea floor, that appears to be sediment-controlled, and may be the steep ice-distal face observed in seismic data from the Greenland margin by *Dowdeswell and Fugelli* [2012]. At the peninsula, there is no lightly grounded plain, such as that found in the embayment, and no region of positive topography underlying the present-day grounding zone is observed.

4.1. Grounding Zone Stability

[14] Grounding zone wedges lead to enhanced drag and a reduction in ice flow [*Alley et al.*, 2007; *Parizek et al.*, 2013]. In this manner, grounding zone deposits can act like any topographic high at the bed. The significance of grounding zone deposits is that they are generated by the ice sheet itself, providing its own topographic stabilization at this critical zone. Our assessment of WIS's grounding zone in these two locations indicates that sedimentation is likely to be occurring in the embayment setting but almost no positive topography is being generated. We note that the timing of the occupation of the current grounding zone position is poorly known [*Conway et al.*, 1999], so we may be imaging an immature grounding zone system.

[15] Accommodation space for grounding zone deposition is determined by both the bathymetric profile and the ice shelf basal profile. The shape of the latter is partly determined by basal melt-rate. Rapid basal melting will lead to

an ice-shelf base that rises steeply in the along-flow direction. A sediment wedge growing to fill this available space will initially have a steep upglacier face. As sediment fills this accommodation space, it will lead to a reduction in basal melting [*Holland*, 2008], the resulting effect being a grounding zone wedge in contact with the overriding ice, providing tangential friction, and stabilizing the grounding zone position. In our case, the ice-shelf roof is nearly horizontal. As a result of this profile, which is likely due to low basal-melt rates in the shallow ocean cavity [*Holland*, 2008], as well as strong ice-shelf buttressing, deposition in the available space does not generate a prominent topographic feature.

[16] The Ross Ice Shelf grounding line has nonetheless been nearly stable over decades despite strong nonsteadiness in flow [*Horgan and Anandakrishnan*, 2006], and the grounding zone in our survey area appears to be strongly stabilized by a local ice-surface high just inland that rises well above flotation (Figures 2a, 2d). We suggest that the mechanism of *Walker et al.* [2013] is active; the tidal rise and fall of the ice shelf leads to muted opposing motions over a flexural wavelength of a few ice thicknesses inland, and this slow cycling tends to compact subglacial sediments in that zone. If so, then sedimentation would fill the sub-ice-shelf cavity with soft sediment that is then compacted and strengthened. We also note the likelihood that the grounding line initially stabilized on a topographic high. This raises the possibility of repeated occupation of the same grounding zone position and stacked grounding zone deposition. It is possible that we observe this in both of our along-flow profiles, where zones of positive topography, with similar characteristics to grounding zone wedges, underlie the modern grounding zone position in the embayment and the pinning point adjacent to the peninsula.

5. Conclusions

[17] Kinematic GPS and active source seismic data acquired across the grounding zone of WIS provide detailed views of this important transition. In an embayment setting, ongoing sedimentation is likely occurring, supporting the style of deposition hypothesized to occur during times of rising sea level by *Alley et al.* [1989]. However, there is currently no large-scale grounding zone wedge in place to stabilize this ice stream against grounding zone retreat [*Alley et al.*, 2007], although processes near the grounding line may have caused sediment compaction contributing to stabilization. Along an adjacent peninsula the grounding zone is proximal to a pinning point and its position is currently maintained by a small step in the subglacial topography.

[18] **Acknowledgments.** This study was supported by the National Science Foundation (NSF-OPP 0424589, 0838763, 0838855) and NASA (NNX-09-AV94G and NNX-10-AI04G). We thank Lucas Beem, Matthew Hill, Rory Hart, Atsuhiro Muto, Benjamin Petersen, and Matthew Siegfried for assistance in the field, Ruzica Dadic for numerous discussions, and Julian A. Dowdeswell and an anonymous reviewer for their constructive comments.

[19] The Editor thanks Julian Dowdeswell and an anonymous reviewer for their assistance in evaluating this paper.

References

Alley, R. B., D. D. Blankenship, C. R. Bentley, and S. T. Rooney (1986), Deformation of till beneath ice stream B, West Antarctica, *Nature*, *322*, 57–59.

Alley, R. B., D. D. Blankenship, C. R. Bentley, and S. T. Rooney (1987), Till beneath ice stream B: 3. Till deformation: Evidence and implications, *J. Geophys. Res.*, *92*(B9), 8921–8929.

Alley, R. B., D. D. Blankenship, S. T. Rooney, and C. R. Bentley (1989), Sedimentation beneath ice shelves—The view from Ice Stream B, *Mar. Geol.*, *85*, 101–120.

Alley, R. B., S. Anandakrishnan, T. Dupont, B. R. Parizek, and D. Pollard (2007), Effect of sedimentation on ice-sheet grounding-line stability, *Science*, *315*(5820), 1838–1841.

Anandakrishnan, S., G. A. Catania, R. B. Alley, and H. J. Horgan (2007), Discovery of till deposition at the grounding line of Whillans Ice Stream, *Science*, *315*(5820), 1835–1838.

Bindschadler, R., et al. (2011), Getting around Antarctica: New high-resolution mappings of the grounded and freely-floating boundaries of the Antarctic ice sheet created for the International Polar Year, *The Cryosphere*, *5*(3), 569–588, doi:10.5194/tc-5-569-2011.

Blankenship, D. D., C. R. Bentley, S. T. Rooney, and R. B. Alley (1986), Seismic measurements reveal a saturated, porous layer beneath an active Antarctic ice stream, *Nature*, *322*, 54–57.

Brunt, K. M., H. A. Fricker, L. Padman, T. A. Scambos, and S. O'Neel (2010), Mapping the grounding zone of the Ross Ice Shelf, Antarctica using ICESat laser altimetry, *Ann. Glaciol.*, *51*(55), 71–79.

Carter, S., and H. A. Fricker (2012), The supply of subglacial meltwater to the grounding line of the Siple Coast, West Antarctica, *Ann. Glaciol.*, *53*(60), 267–280.

Catania, G. A., C. L. Hulbe, and H. Conway (2010), Grounding-line basal melt rates determined using radar-derived internal stratigraphy, *J. Glaciol.*, *56*(197), 545–554.

Chen, G. (1998), GPS kinematics positioning for airbourne laser altimetry at Long Valley, Ph.D. thesis, Massachusetts Institute of Technology.

Christianson, K., R. W. Jacobel, H. J. Horgan, S. Anandakrishnan, and R. B. Alley (2012), Subglacial Lake Whillans—Ice-penetrating radar and GPS observations of a shallow active reservoir beneath a West Antarctic ice stream, *Earth Planet. Sci. Lett.*, *331-332*, 237–245.

Christoffersen, P., S. Tulaczyk, and A. E. Behar (2010), Basal ice sequences in Antarctic ice stream: Exposure of past hydrologic conditions and a principle mode of sediment transfer, *J. Geophys. Res.*, *115* (F03034), 1–12, doi:10.1029/2009JF001430.

Conway, H., B. L. Hall, and G. H. Denton (1999), Past and future grounding-line retreat of the West Antarctic Ice Sheet, *Science*, *286*, 280–283.

Dowdeswell, J. A., and E. M. G. Fugelli (2012), The seismic architecture and geometry of grounding-zone wedges formed at the marine margins of past ice sheets, *Geol. Soc. Am. Bull.*, *124* (11-12), 1750–1761, doi:10.1130/B30628.1.

Fricker, H. A., T. A. Scambos, R. A. Bindschadler, and L. Padman (2007), An active subglacial water system in West Antarctica mapped from space, *Science*, *315*(1544), 1544–1548.

Gomez, N., J. X. Mitrovica, P. Huybers, and P. U. Clark (2010), Sea level as a stabilizing factor for marine-ice-sheet grounding lines, *Nat. Geosci.*, *3*, 850–853.

Gray, L., N. Short, B. Bindschadler, I. Joughin, L. Padman, P. Vornberger, and A. Khananian (2002), Radarsat interferometry for Antarctic grounding zone mapping, *Ann. Glaciol.*, *34*, 269–276.

Haran, T., J. Bohlander, T. Scambos, and M. Fahnestock (2005), *MODIS mosaic of Antarctica (MOA) image map*. NSIDC Digital media.

Holland, P. R. (2008), A model of tidally dominated ocean processes near ice shelf grounding lines, *J. Geophys. Res.*, *113* (C11002), 1–15, doi:10.1029/2007JC004576.

Horgan, H. J., and S. Anandakrishnan (2006), Static grounding lines and dynamic ice streams: Evidence from the Siple Coast, West Antarctica, *Geophys. Res. Lett.*, *33*(L18502), doi:10.1029/2006GL027091.

Horgan, H. J., S. Anandakrishnan, R. W. Jacobel, K. Christianson, R. B. Alley, D. S. Heeszel, S. Picotti, and J. I. Walter (2012), Subglacial Lake Whillans—Seismic observations of a shallow active reservoir beneath a West Antarctic ice stream, *Earth Planet. Sci. Lett.*, *331–332*, 201–209.

Jacobel, R. W., A. E. Robinson, and R. A. Bindschadler (1994), Studies of the grounding-line location in Ice Streams D and E, Antarctica, *Ann. Glaciol.*, *20*, 39–42.

Jamieson, S. S. R., A. Vieli, S. J. Livingstone, C. O. Cofaigh, C. Stokes, C. Hillenbrand, and J. A. Dowdeswell (2012), Ice-stream stability on a reverse slope bed, *Nat. Geosci.*, *6*, 61–64.

Joughin, I., and R. B. Alley (2011), Stability of the West Antarctic ice sheet in a warming world, *Nat. Geosci.*, *4*, 506–513.

Kamb, B. (2001), Basal zone of the West Antarctic ice streams and its role in the lubrication of their rapid motion, in *The West Antarctic Ice Sheet: Behavior and Environment, Antarctic Research Series*, edited by R. B. Alley, and R. A. Bindschadler, pp. 157–200, vol. 77, AGU, Washington, D. C.

MacGregor, J. A., S. Anandakrishnan, G. A. Catania, and D. P. Winebrenner (2011), The grounding zone of the Ross Ice Shelf, West Antarctica, from ice-penetrating radar, *J. Glaciol.*, *57*(205), 917–928.

Parizek, B. R., et al. (2013), Dynamic (in)stability of Thwaites Glacier, West Antarctica, *J. Geophys. Res. Earth Surf.*, *118*(2), 638–655, doi:10.1003/jgrf.20044.

Rignot, E., J. Mouginot, and B. Scheuchl (2011), Antarctic grounding line mapping from differential satellite radar interferometry, *Geophys. Res. Lett.*, *38*(L10504), doi:10.1029/2011GL047109.

Rooney, S. T., D. D. Blankenship, R. B. Alley, and C. R. Bentley (1987), Till beneath ice stream B. 2. Structure and continuity, *J. Geophys. Res.*, *92*(B9), 8913–8920.

Schoof, C. (2007), Ice sheet grounding line dynamics: Steady states, stability and hysteresis, *J. Geophys. Res.*, *112* (F03S28), doi:10.1029/2006JF000664.

Shabtaie, S., and C. R. Bentley (1987), West Antarctic ice streams draining into the Ross Ice Shelf: Configuration and mass balance, *J. Geophys. Res.*, *92*(B2), 1311–1336.

Smith, A. M. (1996), Ice shelf basal melting at the grounding line, measured from seismic observations, *J. Geophys. Res.*, *101*(C10), 22,749–22,755.

Vaughan, D. G. (1995), Tidal flexure at ice shelf margins, *J. Geophys. Res.*, *100*(B4), 6213–6224.

Walker, R. T., B. R. Parizek, R. B. Alley, S. Anandakrishnan, K. L. Riverman, and K. Christinason (2013), Ice-shelf tidal flexure and subglacial pressure variations, *Earth Planet. Sci. Lett.*, *361*, 422–428.

Weertman, J. (1974), Stability at the junction of an ice sheet and an ice shelf, *J. Glaciol.*, *13*, 3–11.